ISEIS

Journal of Environmental Informatics Letters 7(2) 69-79 (2022)

Journal of Environmental Informatics Letters

www.iseis.org/jeil

Impact of Land-Use Dynamics on Land Surface Temperature in Mumbai City, India: A Geospatial Approach

S. Waghchaure[1], R. Vijay[1 *], J. Dey[1,2], and C. Thakre[1,2]

[1]*Wastewater Technology Division, CSIR-National Environmental Engineering Research Institute (NEERI), Nagpur 440020, India*
[2]*Academy of Scientific and Innovative Research (AcSIR), Ghaziabad, Uttar Pradesh 201002, India*

Received 27 January 2022; revised 24 April 2022; accepted 07 June 2017; published online 28 June 2022

ABSTRACT. To assess and monitor the environmental dynamics on a regional or global scale, Land Surface Temperature (LST) has been estimated for South Mumbai, using Landsat data for the years 2000, 2010, 2015, and 2020. The urban heat island (UHI) effect has also been assessed by analysing the LST pattern in the study area. The normalized difference vegetation index (NDVI) analysis shows that LST and UHI effects are less when vegetation cover is high. On the contrary, the normalized difference built-up index (NDBI) is directly proportional to LST which indicates the impact of human activities on LST as well as UHI. The relationship between LST of the study area and ambient air temperature has shown a strong correlation with an increasing trend of LST from 2000 to 2020. The study reveals that the average LST of Mumbai has been increased from 27.1 to 32.7 °C in the last twenty years. The ward-wise temperature profile analysis has been carried out to address the worst thermal discomfort zone and associated population. The study suggests increasing the green space for maintaining the average LST in Mumbai. This study provides a baseline for future studies like LST and human health, climate change, assessment of the ecological status, etc. of the urban environment.

Keywords: green-space, geospatial techniques, land surface emissivity, land surface temperature, urbanization, urban heat island

1. Introduction

Temperature is one of the significant climatic parameters that influenced micro as well as global climate (Baede et al., 2001; Zaksek and Ostir, 2002; Weng, 2009). Literature is telling that the world's temperature is increasing continuously for the last 150 years (Sakhre et al., 2020; Vayssade et al., 2021). In this era of globalization, urbanization especially migration toward the city is increasing drastically. This is the major reason for the alteration of the nature of the land use and land cover (LULC) to fulfill the demands of the country's economic necessities and is also responsible for increasing land surface temperature (LST). The population living in the urban area is more than the rural and it will further increase in upcoming years (United Nations, 2007). Dense residential areas, complex commercial sectors, administrative offices, private trades, concretized roads, and multi-story buildings are the common physiognomies of an urban area. These characteristics make an urban area warmer due to absorption of high solar energy, thermal conductivity, and less reflectivity of the building materials. The formation of urban heat island (UHI) is now a common phenomenon in cities that is also responsible for the increase in urban temperature (Levermore et al., 2017). The haphazard urbanization (Ullah et al., 2019; Kafy et al., 2021) is leading to the effect of the UHI (Saha et al., 2021). The literature reported that vegetation, waterbody, and other classes are replaced by urbanization (Fatemi and Narangifard, 2019; Gohain et al., 2021; Kafy et al., 2021, Mustafa et al., 2021). Therefore, the land-use dynamics especially the increase of the built-up area makes a notable change in LST (Akter et al., 2021; Gazi et al., 2021), as it is strongly influenced by emissivity properties of different LULC classes (Cheng and Liang, 2018). The LST study has great potential for insolation, heat budget, and overall climate change studies (Halder et al., 2021; Salwan et al., 2021; Yang et al., 2021). This climate change has strong contributions to human life and biophysical parameters (Zhang et al., 2021). The increasing trend in LST might be the probable reason for extreme climatic conditions like heat waves and relative stress, drought, irregular rainfall, wildfire, and melting of glaciers, etc. (Babu and Roy, 2020; Buo et al., 2021; Chen and Lin, 2021; Duan et al., 2021; McBean, 2021; Ren et al., 2021; Xie and Fan, 2021).

As temperature is increasing globally (Gogoi et al., 2019), Indian metropolis (Mumbai, Delhi, Kolkata, Chennai) are also experiencing massive changes in surface temperature (Dhorde et al., 2009). The densely populated and highly urbanized city of Mumbai is witnessing an increasing trend in temperature due to the transformation of land use categories (Sahana et al., 2019; Singh and Grover, 2014). In this context, monitoring of LST is necessary as it is related to various environmental issues. It is reported that the increasing public transport, as well as private vehicles, are also responsible for increasing UHI in Mum

* Corresponding author. Tel.: +91-712-224-9402.
E-mail address: r_vijay@neeri.res.in (Ritesh Vijay).

ISSN: 2663-6859 print/2663-6867 online
 doi:10.3808/jeil.202200080

bai (Pacione, 2006). The relocations, unwanted growth of population, transportation, and manufacturing establishments are the main providers of UHI formation.

Geospatial techniques especially thermal remote sensing provide an efficient way to assess and monitor the LST (Quattrochi and Luvall, 2004; Dyras et al., 2005; Weng, 2009).To assess the LST, the utility of thermal remote sensing (Amiri et al., 2009, Mallick et al., 2012, Avdan and Jovanovska 2016) may be addressed as (i) temperature of earth skin matched with calculated data of specific points and it is related to biotic as well as abiotic parameters; (ii) fluctuation of the energy of different land use can influence the LST (Quattrochi and Luvall 1999, Sobrino et al., 2006). Although various satellite data (Zaksek and Ostir, 2002; Weng and Yang, 2004) are available to assess the thermal reflectance of the earth's surface, landsat images were analyzed to calculate the LST as the landsat image has special capabilities to connect the microclimate (Parida et al., 2008; Chakraborty et al., 2014, Khandelwal et al., 2018, Malik and Shukla, 2018) data with the converted temperature data (Southworth, 2004). Therefore the main objecttives of this study are to a) investigate the impacts of LULC dynamics on LST, b) study the relationship between spectral indices and LST, and c) identify the most thermal uncomfortable area with the associated population.

2. Study Area

Mumbai is the capital of Maharashtra state of India located on the west coast of India and serves as the financial center of the country. South Mumbai, popularly known as island city lies between 18° 54' 0" to 19° 03' 0" N and 72° 47' 30" to 72° 53' 0" E with a geographic area of 70 km^2 as shown in Figure 1 South Mumbai consists of nine Community Development (CD) wards for better administration of the city. Mumbai city has a mean elevation of 14 m; the physiographic diversity (presence of hills, and plains) also plays a key role in the dynamics of LST. In Mumbai, the average temperature is recorded as 27 to 30 °C during summer (March to May) and 12 to 19 °C during winter (December to February). This region receives rainfall by the South-Western monsoon and average rainfall is measured as 2,146.6 mm/year.

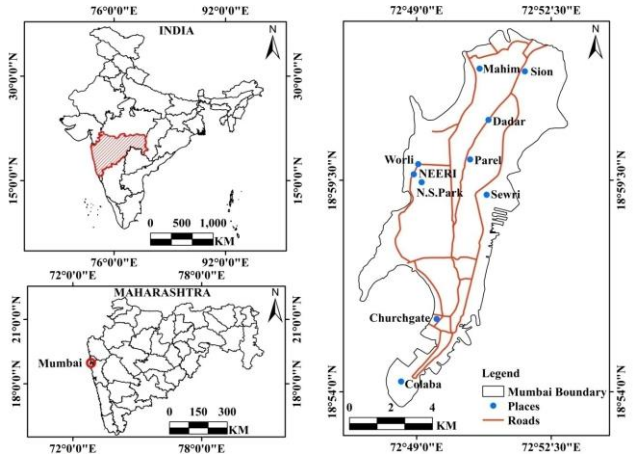

Figure 1. Base-map of the study area.

3. Data and Methods

To carry out the LST study, satellite data were downloaded from the website (https://earthexplorer.usgs.gov/) of the National Aeronautics and Space Administration (NASA). There are four views of false colour composite (FCC) for the Landsat series of satellites (Landsat 5,7,8) obtained over 20 years for the evaluation of the LST of Mumbai city (Figure 2). Landsat-5 (TM) has seven spectral bands of which, band 6 (thermal infrared band) provides the thermal response of the earth's surface feature that was used for the estimation of LST. Other ancillary data like air temperature was collected from the Santacruz regional centre of the Indian Meteorological Department (IMD) (http://www.imdmumbai.gov.in/) and population information from Indian census data of 2011 (https://censusindia.gov.in/2011-common/censusdata2011.html).

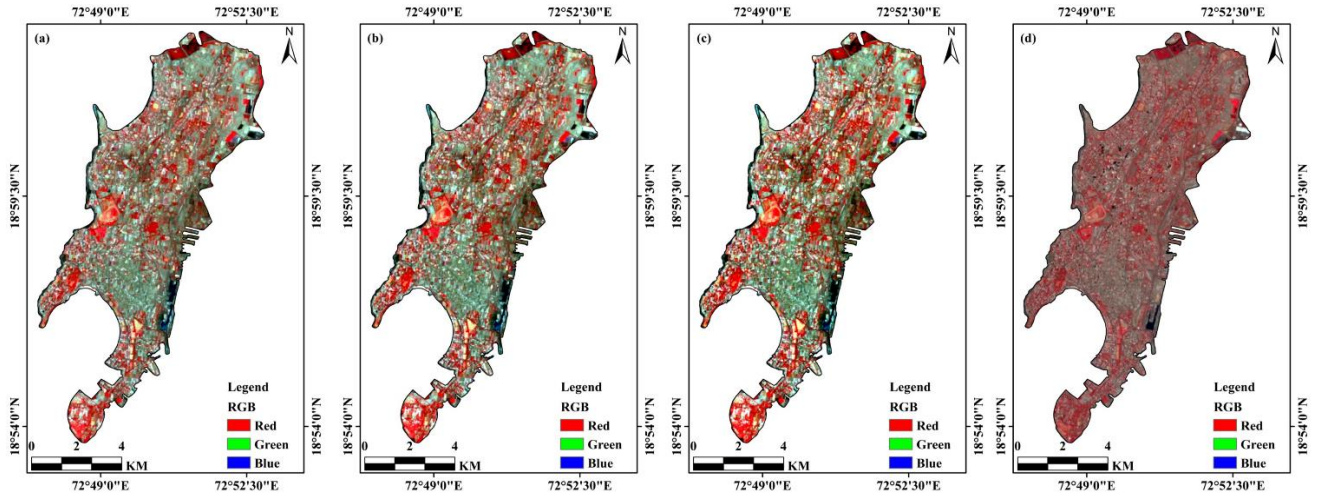

Figure 2. False colour composites (FCCs) of the study area: (a)13 April 2000, (b)17 May 2010, (c) 17 May 2015, and (d) 14 May. 2020).

Table 1. Details of The Satellite Data

Sr. No	Image Acquisition Date	Time
1	13 April 2000	(05:07:49 GMT)
2	17 May 2010	(05:26:08 GMT)
3	17 May 2015	(05:33:17 GMT)
4	14 May 2020	(05:33:45 GMT)

The details of the satellite data have been summarized in Table 1.

The methodology has been described in four sections. Section I describes spectral indices and LULC analysis, Section II deals with land surface emissivity (LSE), Section III is about the retrieval of LST, and Section IV deals with statistical analysis.

3.1 Section I: Spectral Indices and LULC Analysis

Spectral indices are the mathematical approach that uses two or more band combinations to detect an object or classify the image (Vayssade et al., 2021). In this study, the normalized difference vegetation index (NDVI) and normalized difference built-up index (NDBI) have been calculated to assess the importance of these parameters on LST. NDVI analysis helps to understand the reflectance of light changes with chlorophyll content, plant type, and overall ecological conditions of an area. Similarly, NDBI reflects the anthropogenic activities in an area.

The phonological status of different LULC classes may collect through satellite data, as the particular band is responsible to absorb or reflect the specific signal. Based on this concept, NDVI and NDBI ratios were created. The band ratio namely NDVI and NDBI also useful to assess the changes in vegetation cover as well as built-up area. The NDVI and NDBI were calculated using the following algorithms:

$$NDVI = (NIR - Red) / (NIR + Red) \quad (1)$$

$$NDBI = (MIR - NIR) / (MIR + NIR) \quad (2)$$

Time series analysis of LULC provides prior information regarding land-use dynamics in an area. In this study, satellite images were classified into six distinct categories namely built-up, beach, grassland, open land, vegetation, and waterbody. An emphasis has been given to the built-up area because alteration of other land use categories into built-up helps to increase LST (Sakhre et al., 2020). LULC was performed using the maximum likelihood algorithm for supervised classification technique in ERDAS Imagine software.

3.2 Section II: Land Surface Emissivity

According to the emitted radiance, LSE can derive the intrinsic property of every natural object and is a true reflection of the temperature of the earth's surface features (Zhang and Wang, 2008). Emissivity reflects the correlation between the spectral radiance of an object and the temperature of the black body (Artis and Carnahan, 1982; Cheng and Liang 2018). The spectral indices like NDVI have a deep significance (Lo et al., 1997, Klysik and Fortuniak, 1999) to calculate emissivity, as the NDVI helps to classify temperature zones based on the vegetative and non-vegetative coverage (Weng, 2001; Friend, 2002; Chudnovsky et al., 2004) of the surface that may help to minimize the emissivity effects (Weng and Yang, 2004). A relationship between emissivity (e) and NDVI was drawn (Van de Grand and Owe, 1993) using formula number 3 as expressed below:

$$\varepsilon = 1.0094 + 0.047 \times \ln(NDVI) \quad (3)$$

The formula indicates that the results are available in a positive range but it varies from −1 to +1.

3.3 Section III: Retrieval of LST and UHI

The estimation of LST is three steps calculation procedure. The atmospheric correction is the first step, where satellite images were converted into reflectance at the top of the atmosphere (TOA) from its original format of Digital Number (DN) using the equation 4 (NASA 2004, Mallick et al., 2008, Vicente-Serrano et al., 2008, Chander et al., 2009, Sakhre et al., 2020):

$$L\lambda = \left[\left(\frac{Lmax(\lambda) - Lmin(\lambda)}{Qcalmax - Qcalmin}\right) \times (Qcal - Qcalmin)\right] + Lmin(\lambda) \quad (4)$$

where, L_λ is the spectral radiance of sensor aperture in (Watts/m^2·Ster·µm), L_{max} is the spectral radiance that is a scale to Q_{calmax} in (Watts/m^2·Ster·µm), L_{min} is the spectral radiance of scale to Q_{calmin} in (Watts/m^2·Ster·µm), Q_{cal} is the quantized calibrate pixel value of a digital number, Q_{calmax} the maximum quantized calibrate pixel value corresponding to L_{max} in digital number, Q_{calmin} is the minimum quantized calibrate pixel value in digital number. The values for those above-mentioned scale factors and constants are summarised in Table 2.

Table 2. Rescaling Factor and Thermal Constant

Factors	Landsat 5	Landsat 7	Landsat 8
	Band 6	Band 6-2	Band 10
Radiance Maximum Band	15.303	12.650	22.00180
Radiance Minimum Band	1.238	3.200	0.10033
Quantize cal max band	255	255	65535
Quantize cal min band	1	1	1
K_1	607.76	666.09	774.8853
K_2	1,260.56	1,282.71	1,321.0789

Then, the land surface temperature was calculated using an equation (Plank's law) given below (Schott and Volchok,1985):

$$T = \frac{K_2}{\ln\left[\varepsilon_{ix}\frac{K_1}{L\lambda}\right]} - 273.6 \quad (5)$$

where, T represents the temperature (degree Kelvin), and i stands for emissivity. The value of −273.6 was used to get the temperature in degrees Celsius.

The Urban Heat Island (UHI) is a common phenomenon in Mumbai, but there are many cities (e.g., Beijing, Shanghai, etc.) across the globe where the strength of UHI is very high. The presence of coastline, coverage of mangroves, and comparatively lesser altitudes of buildings might be influences the UHI of Mumbai (Singh and Grover, 2014). The UHI in Mumbai city was identified after a critical interpretation of the LST maps.

3.4 Section IV: Statistical Analysis

A temperature profile analysis was carried out (1990 to 2020) using ambient air temperature to understand the fluctuation in air temperature. The temperature profile is a complex time-series data that contained the thermal records about any object or region and it discloses the procedure of recording thermal response and temperature profile analysis. Monthly air temperature variation (minimum, maximum, and average) was performed for the study span (2000 to 2020). To assess the correlation between LST and ambient air temperature for the period of 2000 to 2020, a regression analysis was also performed. Dynamics of LST in different LULC categories for the given period were assessed to understand the importance and balance of LULC to protect the urban climate. Further to assess the thermal discomfort in the wards, LST in each was calculated and compared with the associated population.

4. Results

4.1 Spectral Indices and LULC Analysis

Spectral analysis reveals that the NDVI values are decreasing over the year (Figure 3). Although the minimum and maximum values of NDVI are calculated as −1 and 1, respectively for the study span, the average NDVI is decreasing to 0.12, 0.11, 0.10, 0.09 for the years 2000, 2010, 2015, and 2020, respectively. Unlike NDVI, NDBI is increasing every year (Figure 4). The minimum, maximum and average NDBI values for the years of 2000, 2010, 2015, and 2020 are calculated as −0.37, −0.37, −0.39, and −0.42; 0.46, 0.57, 0.62, and 0.67; 0.08, 0.10, 0.13, and 0.16, respectively.

The changes in LULC are shown in Figure 5, based on the supervised classification of 2000, 2010, 2015, and 2020 satellite images. The dynamics of LULC are inventorized in Figure 6 As far as the areal coverage of vegetation is concerned it is observed that the vegetation is decreasing drastically over the time. In 2000 vegetation cover was 17.9%, but it is decreased by 9.9% by 2020. Similarly, grassland decreased by 0.8% and open land declined by 1.8% from 2000 to 2020. Waterbody is also found in decreasing trend as it is decreasing by 1, 0.3, and 0.1% during 2000 ~ 2010, 2010 ~ 2015, and 2015 ~ 2020, respectively. The beach area has remained unchanged for the study span. Unlike other classes, built-up has increased significantly as 9.1, 1.4, and 3.5% during 2000 ~ 2010, 2010 ~ 2015, and 2015 ~ 2020, respectively with an overall increase of 14%.

4.2 Emissivity, LST and UHI

After estimation of LSE (Figure 7), it is observed that the emissivity range is increasing over the year. The lower limit of LSE is measured as 0.982, 0.984, 0.986, and 0.988 for the years 2000, 2010, 2015, and 2020, respectively. Similarly, the upper value of LSE is also increasing gradually which is quantified as 0.99, 0.992, 0.994, and 0.996 for the years 2000, 2010, 2015, and 2020, respectively. Like LSE, LST (Figure 8) has also been observed in an increasing trend. The LST value is calculated as a minimum of 17.1 , 18.4 , 25.3, and 26.5 ºC; as maximum of 37.1, 37.3, 38.3, and 38.9 ºC; and an average 27.1, 27.8, 31.8, and 32.2 ºC for the years of 2000, 2010, 2015 and 2020, respectively. The inventory of LST (Figure 9) shows that the highest LST range is 35 ~ 38 ºC and the area cover of this range is 9.3% and the highest area cover (25.9%) is under 32 ~ 35 ºC for the year 2000. In 2010, the highest area covered by the LST range (22.9%) is also 32 ~ 35 ºC, but the area covered by the highest tempera- ture range (35 ~ 38 ºC) increased by 17.4%. In 2015 highest area cover is 24.6% by the LST range of 32 ~ 35 ºC but this time upper limit of the LST range is increased to 38 ~ 41ºC and coverage is 9.6%. In 2020 the upper limit of LST is the same with 2015 (38 ~ 41 ºC), but area cover is increased by 11.6%, and the highest area cover is 27.6% by the LST range of 32 ~ 35 ºC.

The UHI effect has been found in multiple places in South Mumbai. The UHI has been focused on the present time and marked on the latest LST map. The five distinct pockets have been marked as prominent UHI in this region as shown in Figure 8d.

4.3 Statistical Analysis

4.3.1. Trends in Temperature

Time series analysis has been performed to assess the variation in maximum, average and minimum temperature in Mumbai city (Figure 10). The graphical representtation indicates a slight increasing trend in maximum and average ambient temperature but a flat trend in minimum temperature.

Similarly, a monthly analysis of temperature data for the years 2000, 2010, 2015, and 2020 (Figure 11) has also been carried out to assess the temperature dynamics. It is observed that after 2000, there is a slight increase in the monthly maximum and average temperature over the years and no significant changes in monthly minimum temperature.

4.3.2. Ward Wise LST

To understand and interpret the LST, ward-wise LST has also been measured. This analysis reflects the detailed and critical measurement of LST. There are nine wards in South Mumbai which is facing considerable variation in temperature

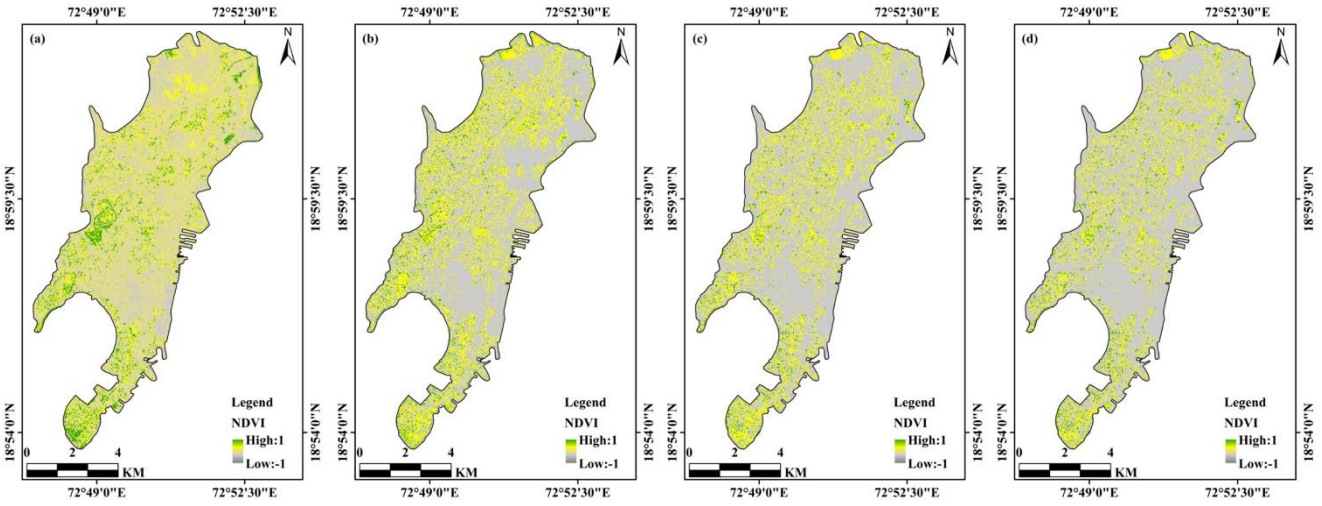

Figure 3. NDVI of the study area (a-13 April 2000, b-17 May 2010, c-17 May 2015, d-14 May 2020).

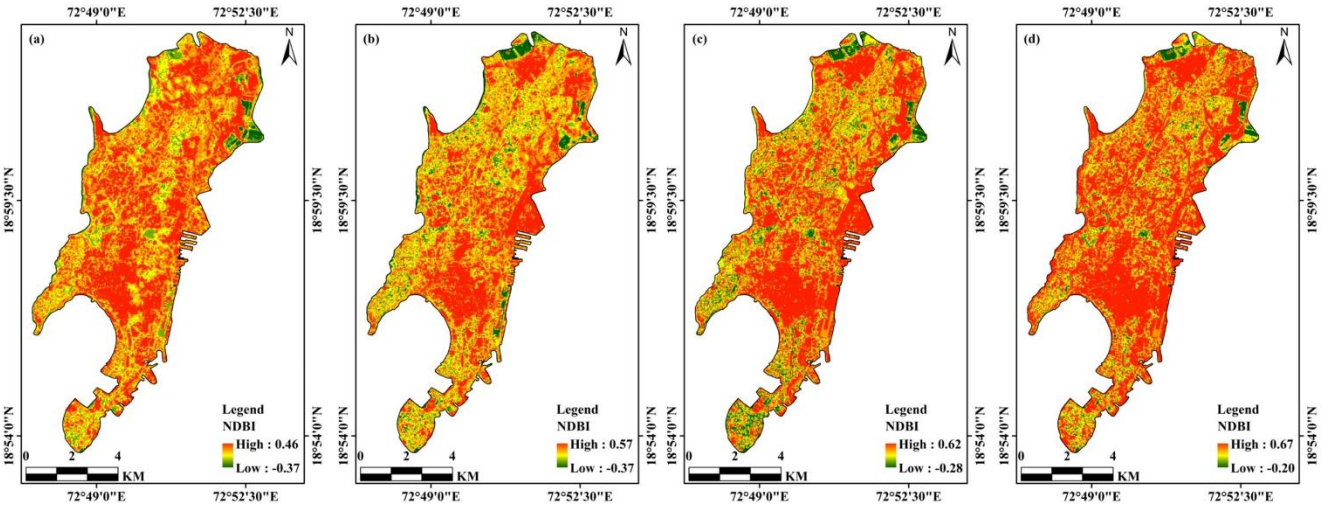

Figure 4. NDBI of the study area on (a) 13 April 2000, (b) 17 May 2010, (c) 17 May 2015, and (d) 14 May 2020.

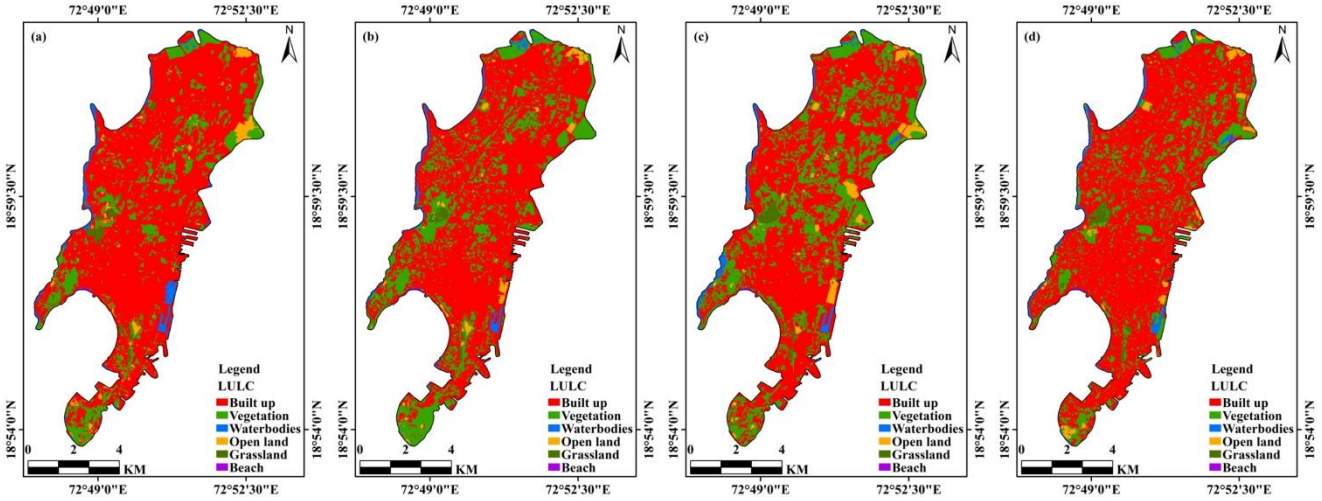

Figure 5. LULC of the study area on (a) 13 April 2000, (b) 17 May 2010, (c) 17 May 2015, and (d) 14 May 2020.

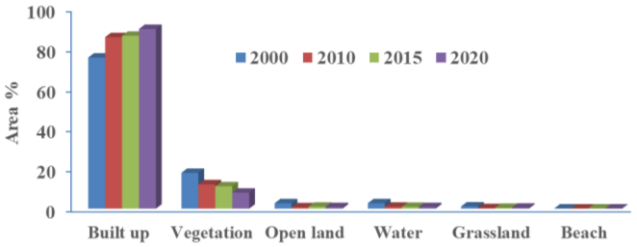

Figure 6. Inventory of LULC.

dynamics. The time series (2000 ~ 2020) analysis of LST for every ward has been represented graphically in Figure 12.

The above graph clearly states that the average LST is always 31 ºC for every ward and ward F/N is facing the highest LST (34.0 ºC) and the highest population (around 6 lakhs). The ward D (31.8 ºC) comes with the lowest LST value (population 3.5 lakhs) for the year 2020. Time series analysis also reveals that LST is continually increasing in the ward F/N. It is observed that in 2000 LST range varied from 23.2 to 31.8 ºC for the ward G/N and C, respectively but in 2020 this range has been calculated as 31.3 to 34.0 ºC for the wards D and F/N, respectively.

LST is sensitive to land use dynamics and it is derived for every LULC class, which is significant to analyze the variation in temperature from 2000 to 2020. Ward wise LST corresponding with different LULC classes such as built up, open land, vegetation, and waterbody has been measured (Figure 13).

Figure 13a indicates that from 2000 to 2020 there is an increase in LST of all the wards due to rapid urbanization. Similarly, Figure 13b is showing the increasing trend in LST in open lands for different wards. The Figure 13c is showing drastic changes in LST in vegetative land that is also proving the decreasing of green cover over the time. The Figure 13d is representing the LST pattern over the watebody, where some of the wards showing increasing in temperature, which might be happening because of reduction in blue space. Some of the wards don't have waterbody class so they are not appearing in the Figure 13d.

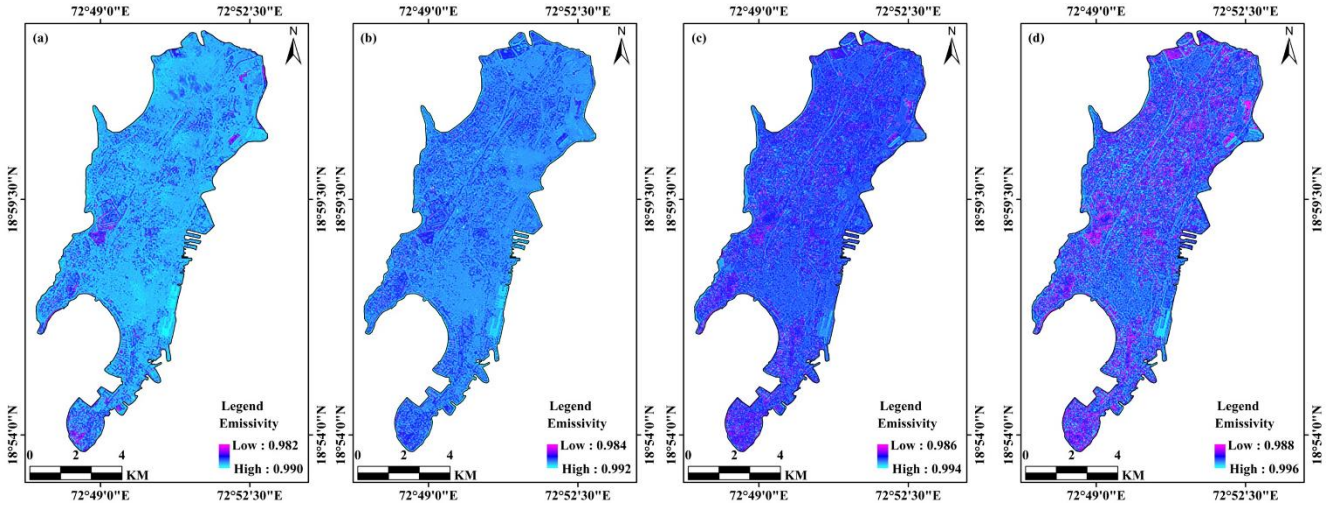

Figure 7. LSE of the study area on (a) 13 April 2000, (b) 17 May 2010, (c) 17 May 2015, and (d) 14 May 2020.

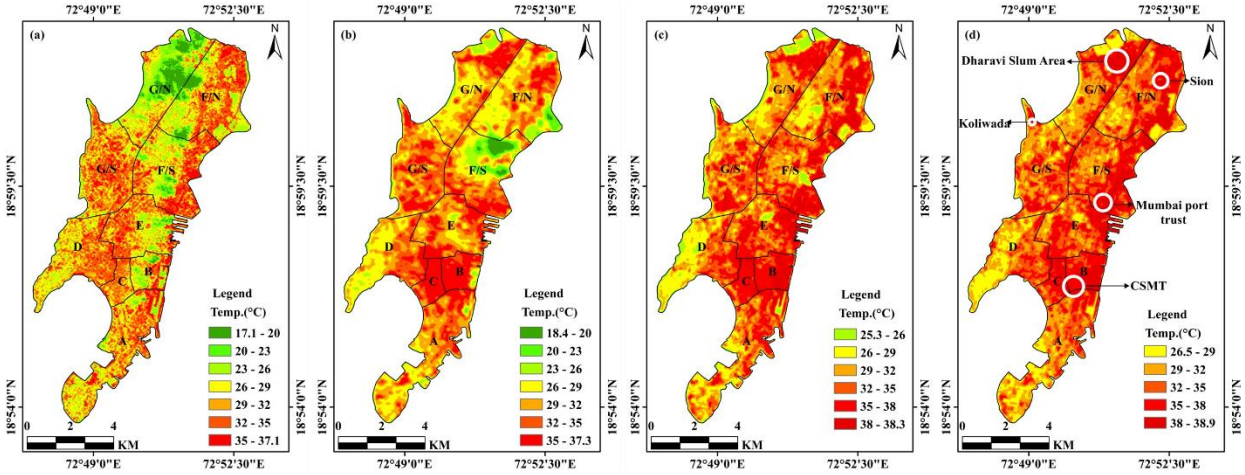

Figure 8. LST of the study area on (a) 13 April 2000, (b) 17 May 2010, (c) 17 May 2015, and (d) 14 May 2020.

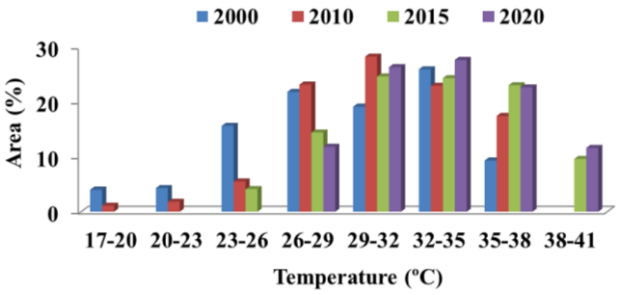

Figure 9. Inventory of LST.

4.4 Relationship between LST and Ambient Air Temperature

A statistical analysis (Figure 14) was carried out to validate the LST with the help of field data collected by the IMD. To carry out this procedure field data with the corresponding months and years has been analyzed. The relationship between average LST of the study area and ambient air temperature shows a strong correlation coefficient of 0.9 with an increasing trend from 2000 to 2020.

5. Discussion

Spectral analysis, more precisely NDVI reflects the ecological value of the city. In this study is observed that the scale of ecological richness is declining over the year, which might have a strong influence on increasing LST. The NDBI shows an increasing trend of anthropogenic activities. Increasing human activities indicates the expansion of impervious surfaces in the city that favors increasing LST. LULC analysis shows declining trends for vegetation, waterbody, grassland, open land, etc. while built-up has increased drastically. The LULC dynamics confirm the replacement of other classes by built-up, which play a crucial role in LST. This increasing trend in LST may be the probable reason for city climate change, UHI heatwave, uncertainty in rainfall patterns, etc. (Gill et al., 2007, Fortuniak ,2009).

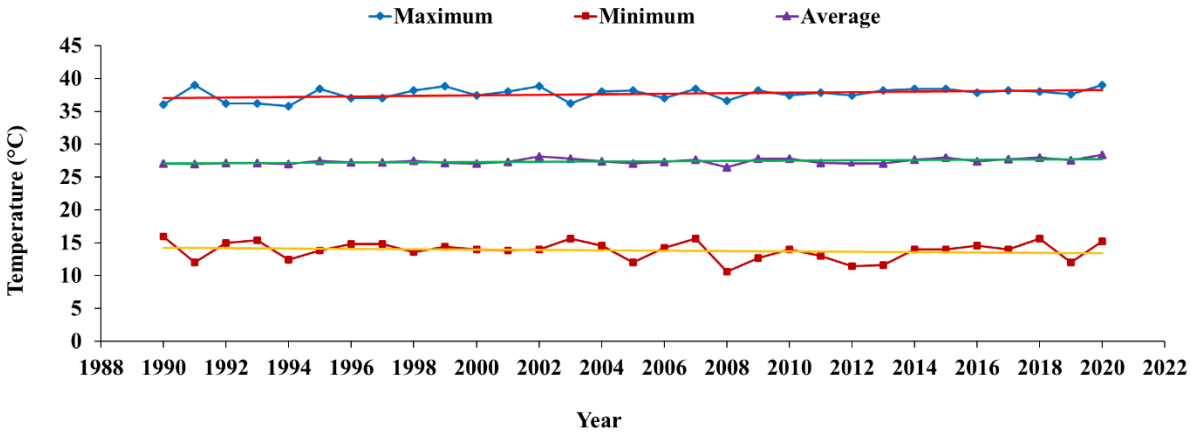

Figure 10. Variation in temperature with time: variation of average maximum-minimum and average measured ambient temperature from 1990 to 2020.

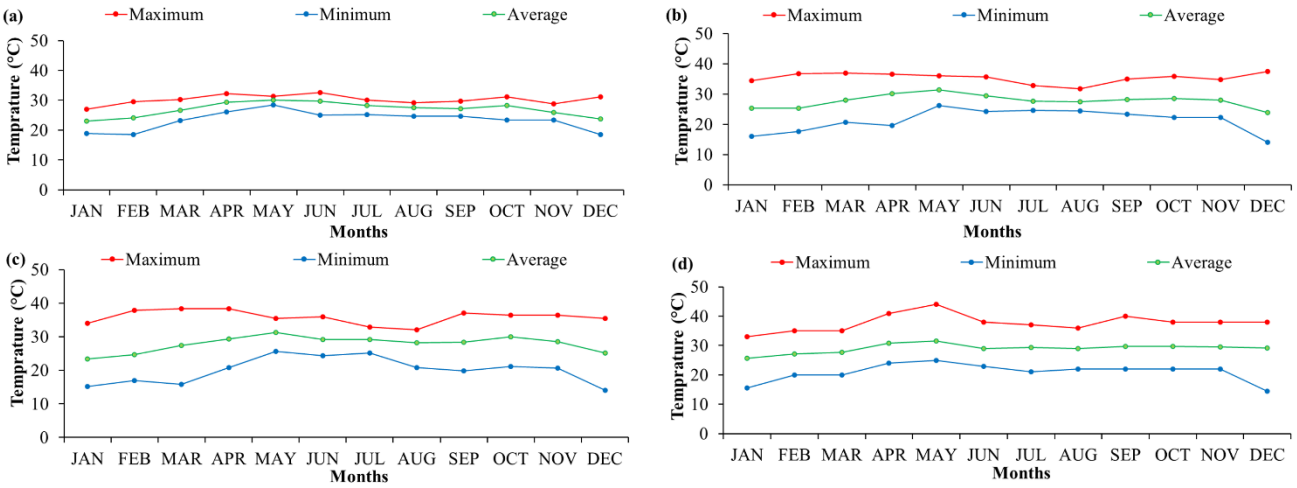

Figure 11. Monthly variation in temperature with time: (a) 2000, (b) 2010, (c) 2015, and (d) 2020.

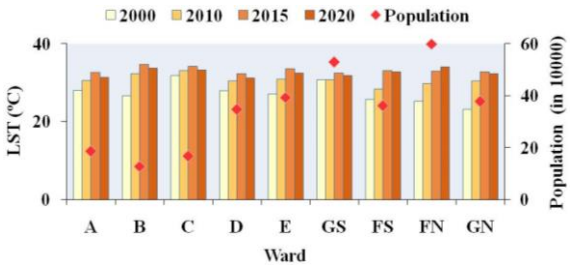

Figure 12. Temperature anomaly in different wards with population.

As emissivity is directly related to the nature of the land use pattern, it also defines an increasing trend, which also supports the increasing LST of South Mumbai. There are significant changes in the lower and upper range of LST from 2000 to 2020 and the areal coverage by the highest temperature zone is increasing, which is showed the spreading of thermal discomfort zones in the city. It is observed that the high density of built-up area along transportation networks (roads, railways) is more responsible for the increase of LST in central Mumbai. The presence of vegetation in the central part and western portions of the city makes it cooler compare with highly urbanized places like Malabar hill, Tardeo, Worli, Colaba, and the north part of the city. It is reported that the evapotranspiration from vegetation may lead to a decrease in the LST as well as ambient air temperature (Yuan and Bauer, 2007). The image analysis results reveal that the mean temperature has risen by 1.9 ℃ in the city. Hence this temperature rise can be attributed by the rise in the built-up of the city.

Some significant pockets have been identified where the UHI effect is prominent. The Dharavi (Asia's largest slum), Juhukoliwada, and Sion slum areas are major highlighted areas as UHI, which might be possible due to dense built-up with less vegetation cover. Other UHI zones like the Bombay port trust area, and Chhatrapati Shivaji Maharaj Terminus (CSMT railway station) are results of increasing LST in the city. Massive traffic (Pacione, 2006), high built up, concretization, and use of machinery indicate the increasing of LST and the effect of UHI in two commercial and transportation regions.

The time-series data reveals that there is an increasing trend in overall temperature. Especially, a linear trend has been found in average temperature over the years. This study is alerting more warming years and uncomfortable situations in upcoming days. The monthly analysis of temperature data reveals that May month is the warmest month throughout the study span. The slight change in temperature for the month of May is addressed as 31.3 to 31.5 ℃ for the years 2000 to 2020, respectively which is evidence in support of the increasing trend in temperature in the present decade. There is an observation on temperature variation that is 1.8 ℃ for average minimum temperature and 3.2 ℃ for mean maximum temperatures.

The ward-wise study of LST has revealed that the population of Mumbai city is facing thermal discomfort. Ward F/N is the living area for the majority of the slum population and is experiencing increasing thermal uneasiness over the year which requires a proper land use policy over there. The ward-wise LST analysis considering the population count living there is an advanced procedure to figure out the actual people who are facing thermal stress and other issues related to this. At the same, the ward-wise study also plays a crucial role in future urban planning, making of land-use policies, and laws. This study is also helpful to find out a way where necessary measures are required to beat the thermal pollution, which will be cooperating on sustainable microclimate.

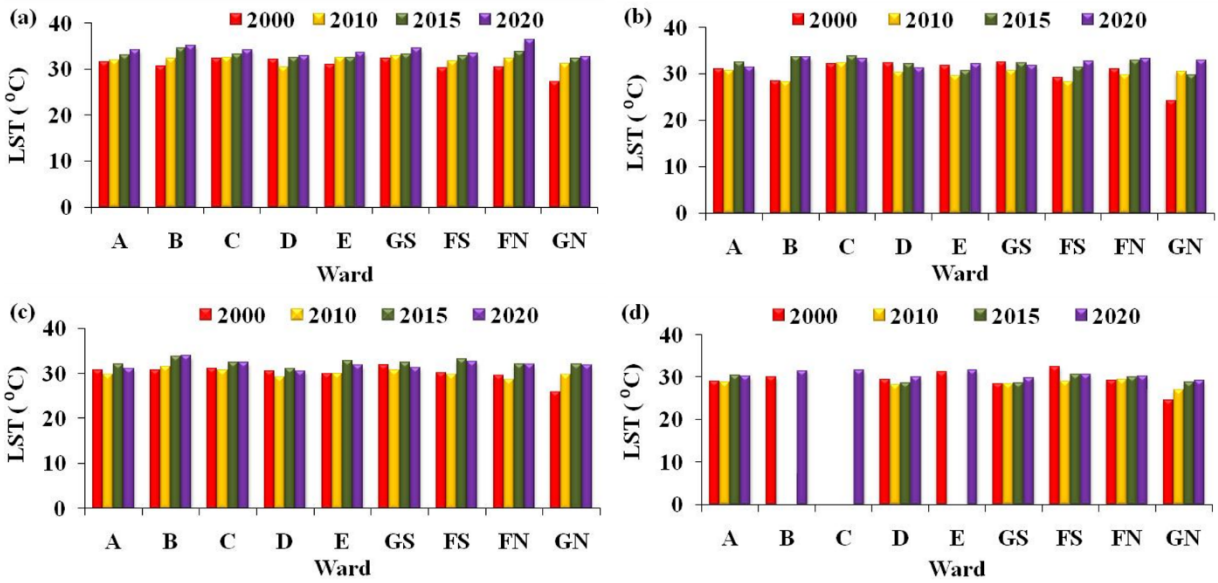

Figure 13. Inventory of particular LULC class and Mean LST: (a) built up, (b) open land, (c) vegetation, and (d) water.

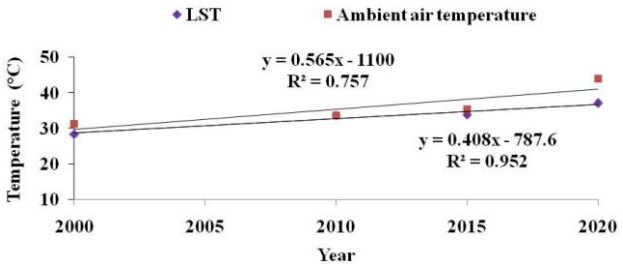

Figure 14. Relation between LST and ambient air temperature: (a) 13 April 2000, (b) 17 May 2010, (c) 17 May 2015, and (d) 14 May 2020

According to the LST and LULC study, built-up pixels were measured the highest in ward F/N and lowest in ward D, which exactly matches ward-wise average LST. Based on this, it is clear that urbanization and LST are directly proportional. Similarly, the LST of the open land category also reveals that the same wards got the position for highest and lowest temperature. In the case of LST of the vegetative portion wards, A and B got the position of lowest and highest temperature, respectively. The increasing of LST in vegetation may address the reduction of density as well as spatial coverage of the green belt in every ward. The increasing trends in LST of every ward disclose the disappearance or shrinking of the waterbody in the wards of Mumbai city.

The statistical analysis is showing a gradual increase in ambient air temperature, which is similar to the LST observations and both are strongly correlated. The trend in temperature dynamics shows evidence of remote sensing analysis that states the increasing temperature with increaseing urbanization. It is reported in the literature that the atmospheric temperature is higher than LST when the temperature of the ambient area is less than zero. The temperature analysis reveals that the temperature of Mumbai is always above zero, which confirms the higher LST than the air temperature.

6. Conclusion

An attempt has been made to assess the significant changes in LULC categories from 2000 to 2020 in Mumbai city and their impact on LST. Spectral indices like NDVI have confirmed the declination of ecological values over the time in the city. NDVI also discloses the disparity in vegetation cover distribution. There are certain places with very less green cover facing high LST. The increasing trend in NDBI shows an expansion of human activities in Mumbai. Thus, LST is directly proportional with NDBI and inversely with NDVI. The LULC analysis shows a significant reduction in vegetation, grassland, water, and open land while built-up has increased drastically. Thus, it is clear that urbanization is taking place over the green-blue space of the city. All these activities are leading to the formation of UHI. The commercial hubs or transport services areas are also responsible for the formation of UHI because of traffic, running of machinery, and building materials that have less reflectivity and more retaining power of heat. The increasing trend in LST and urbanization of corresponding wards may conclude that there is a strong correlation between impervious surfaces and temperature. The LST results were validated with field data collected from IMD showing a strong correlation between them that indicates the importance of remote sensing data to estimate the LST and related environmental issues. This study also delineated the most affected places in terms of wads and living populations who are facing thermal discomfort. The findings of the study are useful for the governments, municipalities, city planners, and policymakers to pay attention towards an effective strategy for sustainable land use for the betterment of citizen's life as well as a stable urban climate. The study recommends an increase in green space in the form of social forest, vegetation, a plantation along the roads, and highways, mandatory green coverage at the residential colony, and office premises to maintain and control of average LST in Mumbai city. This study also focuses on further research on the impact of LST on human health, effective land-use policy for improving resident's life and sustainable urban climate, etc.

Acknowledgment. The authors are thankful to the Director CSIR–National Environmental Engineering Research Institute, Nagpur, for providing the necessary infrastructure and support for carrying out this research study.

References

Akter, T., Gazi, M. and Mia, M. (2021). Assessment of land cover dynamics, land surface temperature, and heat island growth in northwestern Bangladesh using satellite imagery. *Environmental Processes*, 8(2), 661-690. https://doi.org/10.1007/s40710-020-00491-y

Amiri, R., Weng, Q., Alimohammadi, A. and Alavipanah, S.K. (2009). Spatial-temporal dynamics of land surface temperature in relation to fractional vegetation cover and land use/cover in the Tabriz urban area. *Remote Sensing of Environment*, 113(12), 2606-2617. https://doi.org/10.1016/j.rse.2009.07.021

Artis, D.A. and Carnahan, W.H. (1982). Survey of emissivity variability in thermography of urban areas. *Remote Sensing of Environment*, 12(4), 313-329. https://doi.org/10.1016/0034-4257(82)90043-8

Avdan, U. and Jovanovska, G. (2016). Algorithm for automated mapping of the land surface temperature using Landsat 8 satel- lite data. *Journal of Sensors*, 2016, 1-8. https://doi.org/10.1155/2016/14 80307

Babu, K. and Roy, A. (2020). Static fire danger estimation based on the historical MODIS hotspot data using geospatial techniques for the uttarakhand state, India. *International Society for Environmental Information Science*, 4(1), 11-21. https://doi.org/10.3808/jeil.202000038

Baede, D.S., M, A.P., Ahlonsou, E., Ding, Y. and Bolin, S.P.B. (2001). The Climate system: an overview. In: Houghton JT. Climate Change 2001: The scientific basis. IPCC, Cambridge University Press, Cambridge, pp 51-64.

Buo, I., Sagris, V. and Jaagus, J. (2021). Gap-filling satellite land surface temperature over heatwave periods with machine learning. *IEEE Geoscience and Remote Sensing Letters*, 19, 1-5. https://doi.org/10.1109/LGRS.2021.3068069

Chakraborty, S.D., Kant, Y. and Bharath, B.D. (2014). Study of land surface temperature in Delhi city to manage the thermal effect on urban developments. *International journal of advanced scientific*

and technical research, 4(1), 439-450.

Chen, T.L. and Lin, Z.H. (2021). Impact of land use types on the spatial heterogeneity of extreme heat environments in a metropoli- tan area. *Sustainable Cities and Society*, 72(4), 103005. https://doi.org /10.1016/j.scs.2021.103005

Chander, G., Markham, B.L. and Helder, D.L. (2009). Summary of current radiometric calibration coefficients for Landsat MSS, TM, ETM+, and EO-1 ALI sensors. *Remote Sensing of Environment*, 113(5), 893-903. https://doi.org/10.1016/j.rse.2009.01.007

Cheng, J. and Liang, S. (2018). Land-surface emissivity. *Comprehensive Remote Sensing*, 5, 217-263. https://doi.org/10.1016/B9 78-0-12-409548-9.10374-4

Chudnovsky, A., Ben-Dor, E. and Saaroni, H. (2004). Diurnal thermal behavior of selected urban objects using remote sensing measurements. *Energy and Buildings*, 36(11), 1063-1074. https: //doi.org/10.1016/j.enbuild.2004.01.052

Dhorde, A., Dhorde, A., and Gadgil, A.S. (2009). Long-term temperature trends at four largest cities of India during the twentieth century. *The Journal of Indian Geophysical Union*, 13(2), 85-97.

Duan, R., Huang, G., Li, Y., Zhou, X., Ren, J. and Tian, C. (2021). Stepwise clustering future meteorological drought projection and multi-level factorial analysis under climate change: A case study of the Pearl River Basin, China. *Environmental Research*, 196, 110368. https://doi.org/10.1016/j.envres.2020.110368

Dyras, I., Dobesch, H., Grueter, E., Perdigao, A., Tveito, O.E., Thornes, J.E., van der Wel, F. and Bottai, L. (2005). The use of geographic information systems in climatology and meteorology. *Meteorological Applications*, 12(1), 1-5. https://doi.org/10.1017/ S1350482705001544

Fatemi, M. and Narangifard, M. (2019). Monitoring LULC changes and its impact on the LST and NDVI in District 1 of Shiraz City. *Arabian Journal of Geosciences*, 12(4), 1-12. https://doi.org/10. 1007/s12517-019-4259-6

Fortuniak, K. (2009). Global environmental change and urban climate in Central European cities. *The environmental and socio-economic response in the southern Baltic region, Proc. of International Conference on Climate Change.* Szczecin, Poland, 65-66.

Friend, M.A. (2002). Forward and inverse modeling of land surface energy balance using surface temperature measurements. *Remote Sensing Environment*, 79(2-3), 344-354. https://doi.org/10.1016/S 0034-4257(01)00284-X

Gazi, M., Rahman, M., Uddin, M. and Rahman, F.M. (2021). Spatio-temporal dynamic land cover changes and their impacts on the urban thermal environment in the Chittagong metropolitan area, Bangladesh. *GeoJournal*, 86(5), 2119-2134. https://doi.org/10.100 7/s10708-020-10178-4

Gill, S.E., Handley, J.F., Ennos, A.R. and Pauleit, S. (2007). Adapting cities for climate change: the role of the green infrastructure. *Built Environment*, 33(1), 115-133. https://doi.org/10.2148/benv.3 3.1.115

Gogoi, P.P., Vinoj, V., Swain, D., Roberts, G., Dash, J. and Tripathy, S. (2019). Land use and land cover change effect on surface temperature over Eastern India. *Scientific Reports*, 9(1), 1-10. http s://doi.org/10.1038/s41598-019-45213-z

Gohain, K.J., Mohammad, P. and Goswami, A. (2021). Assessing the impact of land use land cover changes on land surface temperature over Pune city, India. *Quaternary International*, 575-576, 259-269. https://doi.org/10.1016/j.quaint.2020.04.052

Halder, B., Bandyopadhyay, J. and Banik, P. (2021). Evaluation of the climate change impact on urban heat island based on land surface temperature and geospatial indicators. *International Journal of Environmental Research*, 15(5), 819-835. https://doi.org/10.1007 /s41742-021-00356-8

Kafy, A.A., Faisal, A.A., Shuvo, R.M., Naim, M.N.H., Sikdar, M.S., Chowdhury, R.R., Islam, M.A., Sarker, M.H.S., Khan, M.H.H. and Kona, M.A. (2021). Remote sensing approach to simulate the land use/land cover and seasonal land surface tem- perature change using machine learning algorithms in a fastest-growing megacity of Bangladesh. *Remote Sensing Applications: Society and Environment*, 21, 100463. https://doi.org/10.1016/j.rsase.2020. 100463

Kafy, A.A., Rakib, A.A., Akter, K.S., Rahaman, Z.A., Faisal, A.A., Mallik, S., Nasher, N.R., Hossain, M.I. and Ali, M.Y. (2021). Monitoring the effects of vegetation cover losses on land surface temperature dynamics using geospatial approach in Rajshahi city, Bangladesh. *Environmental Challenges*, 4, 100187. https://doi.org /10.1016/j.envc.2021.100187

Khandelwal, S., Goyal, R., Kaul, N. and Mathew, A. (2017). Assessment of land surface temperature variation due to change in elevation of the area surrounding Jaipur, India. *The Egyptian Journal of Remote Sensing and Space Science*, 21(1), 87-94. https:// doi.org/10.1016/j.ejrs.2017.01.005

Klysik, K. and Fortuniak, K. (1999). Temporal and spatial characteristics of the urban heat island of Lodz, Poland. *Atmospheric Environment*, 33(24-25), 3885-3895. https://doi.org/10. 1016/S1352-2310(99)00131-4

Lo, C.P., Quattrochi, D.A. and Luvall, J.C. (1997). Application of high-resolution thermal infrared remote sensing and GIS to assess the urban heat island effect. *International Journal of Remote Sensing*, 18(2), 287-304. https://doi.org/10.1080/014311697219079

McBean, E.A. (2021). Global climate change: assessing the importance of the roles of ice cover and glacial changes. *Journal of Environmental Informatics Letters*, 5(2), 68-74. https://doi.org/10.38 08/jeil.202100061

Malik, M.S. and Shukla, J.P. (2018). Retrieving of the land surface temperature using thermal remote sensing and GIS techniques in Kandaihimmat Watershed, Hoshangabad, Madhya Pradesh. *Journal of the Geological Society of India*, 92(3), 298-304. https:// doi.org/10.1007/s12594-018-1010-y

Mallick, J., Kant, Y. and Bharath, B.D. (2008). Estimation of land surface temperature over Delhi using Landsat-7 ETM+. *Journal of Indian Geophysical Union*, 12(3), 131-140.

Mallick, J., Singh, C.K., Shashtri, S., Rahman, A. and Mukherjee, S. (2012). Land surface emissivity retrieval based on moisture index from LANDSAT TM satellite data over heterogeneous surfaces of Delhi city. *International Journal of Applied Earth Observation and Geoinformation*, 19, 348-358. https://doi.org/10.1016/j.jag.20 12.06. 002

Mustafa, E.K., Liu, G., El-Hamid, A., Hazem, T. and Kaloop, M.R. (2021). Simulation of land use dynamics and impact on land surface temperature using satellite data. *GeoJournal*, 86(3), 1089-1107. https://doi.org/10.1007/s10708-019-10115-0

NASA. (2004). Landsat Project Science Office: Landsat 7 Science data users handbook, Chapter: 11, Data Products. https://www. gsfc.nasa.gov/IAS/handb ook/handbook_htmls

Pacione, M. (2006). City profile: Mumbai. *Cities*, 23(3), 229-238. https://doi.org/10.1016/j.cities.2005.11.003

Parida, B.R., Oinam, B., Patel, N.R., Sharma, N., Kandwal, R. and Hazarika, M.K. (2008). Land surface temperature variation in relation to vegetation type using MODIS satellite data in Gujarat state of India. *International Journal of Remote Sensing*, 29(14), 4219-4235. https://doi.org/10.1080/01431160701871096

Quattrochi, D.A. and Luvall, J.C. (1999). Thermal infrared remote sensing data for analysis of landscape ecological processes: Methods and applications. *Landscape Ecology*, 14(6), 577-598. https:// doi.org/10.1023/A:1008168910634

Quattrochi, D.A. and Luvall, J C. (2003). Thermal remote sensing in land surface processes. CRC Press, pp 1-464. https://doi.org/10.12 01/9780203502174

Ren, J., Huang, G., Li, Y., Zhou, X., Lu, C. and Duan, R. (2021). Stepwise-clustered heatwave downscaling and projection for Guangdong Province. *International Journal of Climatology*, 42(5),

2835-2860. https://doi.org/10.1002/joc.7393

Saha, S., Saha, A., Das, M., Saha, A., Sarkar, R. and Das, A. (2021). Analyzing spatial relationship between land use/land cover (LULC) and land surface temperature (LST) of three urban agglomerations (UAs) of Eastern India. *Remote Sensing Applications: Society and Environment*, 22, 100507. https://doi.org/10.1016/j.rsase.2021.100507

Sahana, M., Dutta, S., and Sajjad, H. (2019). Assessing land transformation and its relation with land surface temperature in Mumbai city, India using geospatial techniques. *International Journal of Urban Sciences*, 23(2), 205-225. https://doi.org/10.1080/12265934.2018.1488604

Sakhre, S., Dey, J., Vijay, R. and Kumar, R. (2020). Geospatial assessment of land surface temperature in Nagpur, India: an impact of urbanization. *Environmental Earth Sciences*, 79(10), 226. https://doi.org/10.1007/s12665-020-08952-1

Salwan, A.A., Ahmed, A.A. and Salim, M.A. (2021). Using ArcGIS software and remote sensing technology to predict land surface temperature (LST) for monitoring ecological and climate change in Hor Al-Dalmaj, southern Iraq. *IOP Conference Series: Earth and Environmental Science*, 790(1), 012076. https://doi.org/10.1088/1755-1315/790/1/012076

Schott, J.R. and Volchok, W.J. (1985). Thematic mapper thermal infrared calibration. *Photogrammetric Engineering and Remote Sensing*, 51(9), 1351-1357.

Singh, R.B. and Grover, A. (2014). Remote sensing of urban microclimate with special reference to urban heat island using Landsat thermal data. *Geographia Polonica*, 87(4), 555-568. https://doi.org/10.7163/GPol.2014.38

Sobrino, J.A., Jimenez-Munz, J.C., Zarco-Tejada, P.J., Sepulcre-Canto, G. and Miguel, E. (2006). Land surface temperature derived from airborne hyperspectral scanner thermal infrared data. *Remote Sensing of Environment*, 102(1-2), 99-115. https://doi.org/10.1016/j.rse.2006.02.001

Southworth, J. (2004). An assessment of Landsat TM band 6 thermal data for analyzing land cover in tropical dry forests. *International Journal of Remote sensing*, 25(4), 689-706. https://doi.org/10.1080/ 0143116031000139917

Ullah, S., Ahmad, K., Sajjad, R.U., Abbasi, A.M., Nazeer, A. and Tahir, A.A. (2019). Analysis and simulation of land cover changes and their impacts on land surface temperature in a lower Himalayan region. *Journal of Environmental Management*, 245, 348-357. https://doi.org/10.1016/j.jenvman.2019.05.063

United Nations (2007). *World Urbanization Prospects*. The 2007 Revision Population Database.

van de Griend, A.A., and OWE, M. (1993). On the relationship between thermal emissivity and the normalized difference vegetation index for natural surfaces. International Journal of remote sensing, 14(6), 1119-1131. https://doi.org/10.1080/0143 1169308904400

Vayssade, J.A., Paoli, J.N., Gée, C. and Jones, G. (2021). DeepIndices: remote sensing indices based on approximation of functions through deep-learning, application to uncalibrated vegetation images. *Remote Sensing*, 13(12), 2261. https://doi.org/10.3390/rs13122261

Vicente-Serrano, S.M., Pérez-Cabello, F. and Lasanta, T. (2008). Assessment of radiometric correction techniques in analyzing vegetation variability and change using time series of Landsat images. *Remote Sensing of Environment*, 112(10), 3916-3934. https://doi.org/10.1016/j.rse.2008.06.011

Wan, Z., Wang, P. and Li, X. (2004). Using MODISLand surface temperature and normalized difference vegetation index products for monitoring drought in the southern great plains, USA. *International Journal of Remote sensing*, 25(1), 61-72. https://doi.org/10.1080/0143116031000115328

Weng, Q. (2009). Thermal infrared remote sensing for urban climate and environmental studies: methods, applications, and trends. *ISPRS Journal of Photogrammetry and Remote Sensing*, 64(4), 335-344. https://doi.org/10.1016/j.isprsjprs.2009.03.007

Weng, Q. and Yang, S. (2004). Managing the adverse thermal effects of urban development in a densely populated Chinese city. *Journal of Environmental Management*, 70(2), 145-156. https://doi.org/10.1016/j.jenvman.2003.11.006

Weng, Q. (2001). Remote sensing-GIS evaluation of urban expansionand its impact on surface temperature in the Zhujiang Delta China. *International Journal of Remote Sensing*, 22(10), 1999-2014. https://doi.org/10.1080/713860788

Xie, F. and Fan, H. (2021). Deriving drought indices from MODIS vegetation indices (NDVI/EVI) and Land Surface Temperature (LST): Is data reconstruction necessary? *International Journal of Applied Earth Observation and Geoinformation*, 101, 102352. https://doi.org/10.1016/j.jag.2021.102352

Yang, M., Zhao, W., Zhan, Q. and Xiong, D. (2021). Spatiotemporal patterns of land surface temperature change in the tibetan plateau based on MODIS/Terra daily product from 2000 to 2018. *IEEE Journal of Selected Topics in Applied Earth Observations and Remote Sensing*, 14, 6501-6514. https://doi.org/10.1109/JSTARS.2021.3089851

Yuan, F. and Bauer, M.E. (2007). Comparison of impervious surface area and normalized difference vegetation index as indicators of surface urban heat island effects in Landsatimagery. *Remote Sensing of Environment*, 106(3), 375-386. https://doi.org/10.1016/j.rse.2006.09.003

Zaksek, K. and Ostir, K. (2002). Downscaling land surface temperature for urban heat island diurnal cycle analysis. *Remote Sensing of Environment*, 117, 114-124. https://doi.org/10.1016/j.rse.2011.05.027

Zhang, J. and Wang, Y. (2008). Study of the relationships between the spatial extent of surface urban heat islands and urban characteristic factors based on lands at ETM+ data. *Sensors*, 8(11), 7453-7468. https ://doi.org/10.3390/s8117453

Zhang, W., Luo, G., Chen, C., Ochege, F.U., Hellwich, O., Zheng, H., Hamdi, R. and Wu, S. (2021). Quantifying the contribution of climate change and human activities to biophysical para- meters in an arid region. *Ecological Indicators*, 129, 107996. https://doi.org/10.1 016/j.ecolind.2021.107996